

PULSE CODE TRANSFORMATIONS ON AXONAL TREES*

ALWYN C. SCOTT

*Center for Nonlinear Studies, Los Alamos National Laboratory,
Los Alamos, New Mexico 87545, U.S.A.*

and

UJA VOTA-PINARDI

*Laboratorio di Cibernetica, Via Toiana 2,
Arco Felice (Napoli), Italy.*

(Received June 19, 1982)

Abstract

Exploratory observations of pulse code transformations on giant axons of the squid are reported. Differential transformations which depend upon pulse speed variation with pulse interval (i.e. dispersion) are shown to be governed by a general dispersion relation. Quantum pulse code transformations which involve the loss of entire pulses at axonal bifurcations are related to branch geometry. Quantum transformations were observed only in the strongly dispersive range of pulse interval.

1. Introduction

Since 1952 when a 'quantitative description of membrane current' was published by Hodgkin and Huxley (1952), a credible biophysics of nerve impulse dynamics has been actively developing (Scott, 1977). Progress in the applied mathematics of reaction-diffusion systems and a dramatic increase in computing power have supported the growing experimental skills and insights of electrophysiologists, leading them to ask ever more penetrating questions about the dynamics of nerve impulse interactions. Particularly interesting have been suggestions that certain neurons may perform more complex information processing than a simple linear threshold computation (Waxman, 1972; Scott, 1977, Ch. 6).

With respect to such suggestions, we see two types of question or levels of consideration. The first is to ask whether a certain effect is physiologically possible and, given a positive reply, the second is to ask whether this effect is used in the normal functioning of a real neural system. The first is a question of biophysics, the second is biology *per se*. Our motivation in the work to be described here is to ask the first type of question about information processing in neural systems. More specifically we ask: What are the physiological parameters that describe and limit processes of pulse code transformations on nerve fibers?

* The experimental work was performed at the Stazione Zoologica of Naples.

Our initial experiments have been performed on straight axons and branching preparations from the squid. On straight axons we have studied differential pulse code transformations (DPT) which are caused by 'dispersion' or pulse velocity variations that depend upon local values of the pulse interval. With branching preparations we were able to study quantum pulse code transformations (QPT) which involve the sudden loss (or gain) of an action potential, the quantum unit of neural information. Our aim in the study of QPT was to relate dynamic effects to fiber geometry, so the experiments were arranged to minimize the effects of changes in ionic concentrations.

2. Materials and methods

Experiments reported here were with the squid (*Loligo vulgaris*) collected from the Bay of Naples and kept in an aquarium with filtered, constantly running sea water for no more than one week. In order to obtain the preparation for our experiments, the squid was decapitated and immediately placed in cold sea water; then we cut the ventral zone of the mantle completely from one end to the other and removed all internal organs and the two fins. Prepared in this way the mantle was fixed with pins in the dissecting basin in cold sea water (6–12°C) above an illuminating panel. At this point the operation continued under a stereomicroscope. The giant axon was cut just where it leaves the stellate ganglion and immediately tied to avoid loss of axoplasm. Using techniques for microdissection, we removed part of the muscle and connective tissue creating a furrow and cutting all of the small lateral branches as far as possible from the main axon. The axon, now free, was carefully removed from the furrow as far as a large bifurcation the branches of which were removed in a similar way and tied. Fig. 1 shows a typical mantle after both of the giant axons plus three bifurcations have been removed. These axons start out from the stellate ganglion and run through connective tissue for a centimeter or two before entering the mantle and leaving a visible trace on Fig. 1. Several bifurcations are displayed in Fig. 2 which shows a variety of ratios between smaller and larger daughter branches. In 7–5–80B the two daughters are almost equal while in 19–5–80B the larger daughter has several times the diameter of the smaller. Between the stellate ganglion and a bifurcation, several small lateral branches are observed with diameters between 30 and 100 microns and a linear density of about 0.26 per millimeter.

During measurements the axon and bifurcation were pinned to a microscope slide covered with Sylgard resin and placed in a plastic chamber through which sea water was circulated from a cooled (or heated) 500 ml reservoir. Oxygen was bubbled slowly into the chamber before and during the measurements. Stimulation (S) was by any of three methods: external parallel wire (platinum) electrodes, an external suction electrode, or an internal glass microelectrode. Registration was entirely by internal glass microelectrodes filled with 3M-KCl

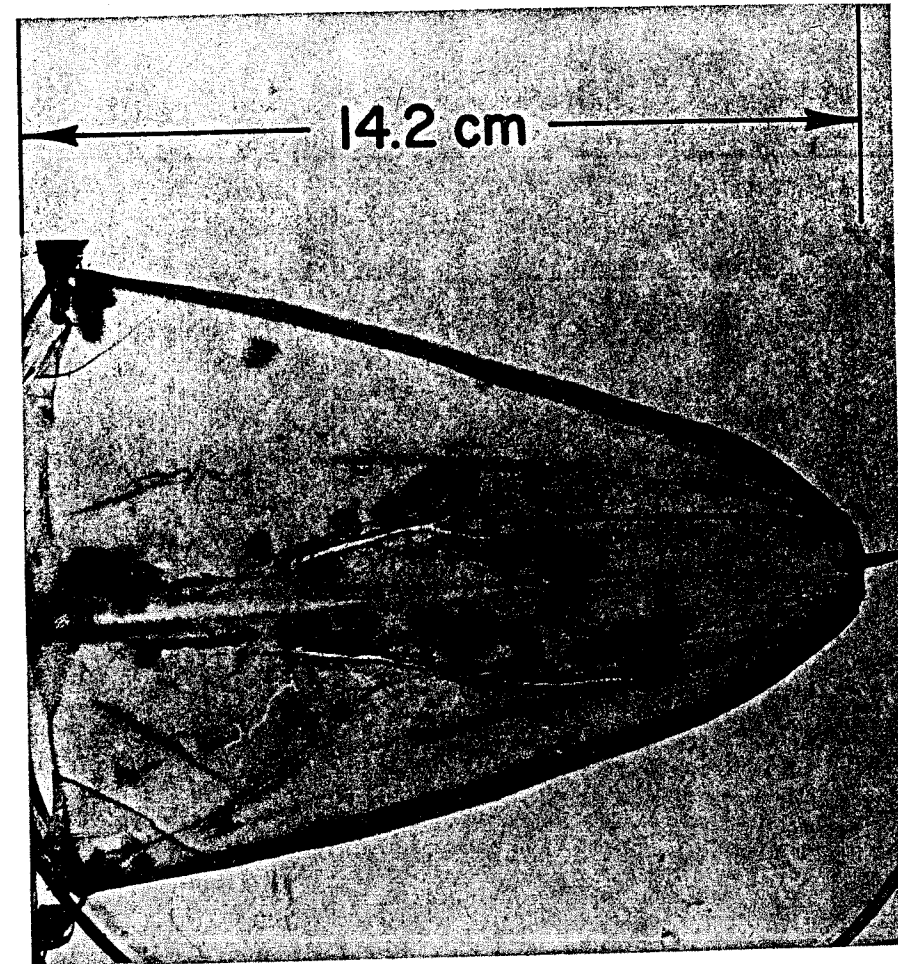


Fig. 1. The mantle of a typical squid after removal of two giant axons and three branches.

and selected for low resistance (5–20 M Ω). Signals from the microelectrodes were presented to high input impedance preamplifiers connected to a Tektronix 565 oscilloscope, and stimulation was obtained from a Grass S88 pulse generator.

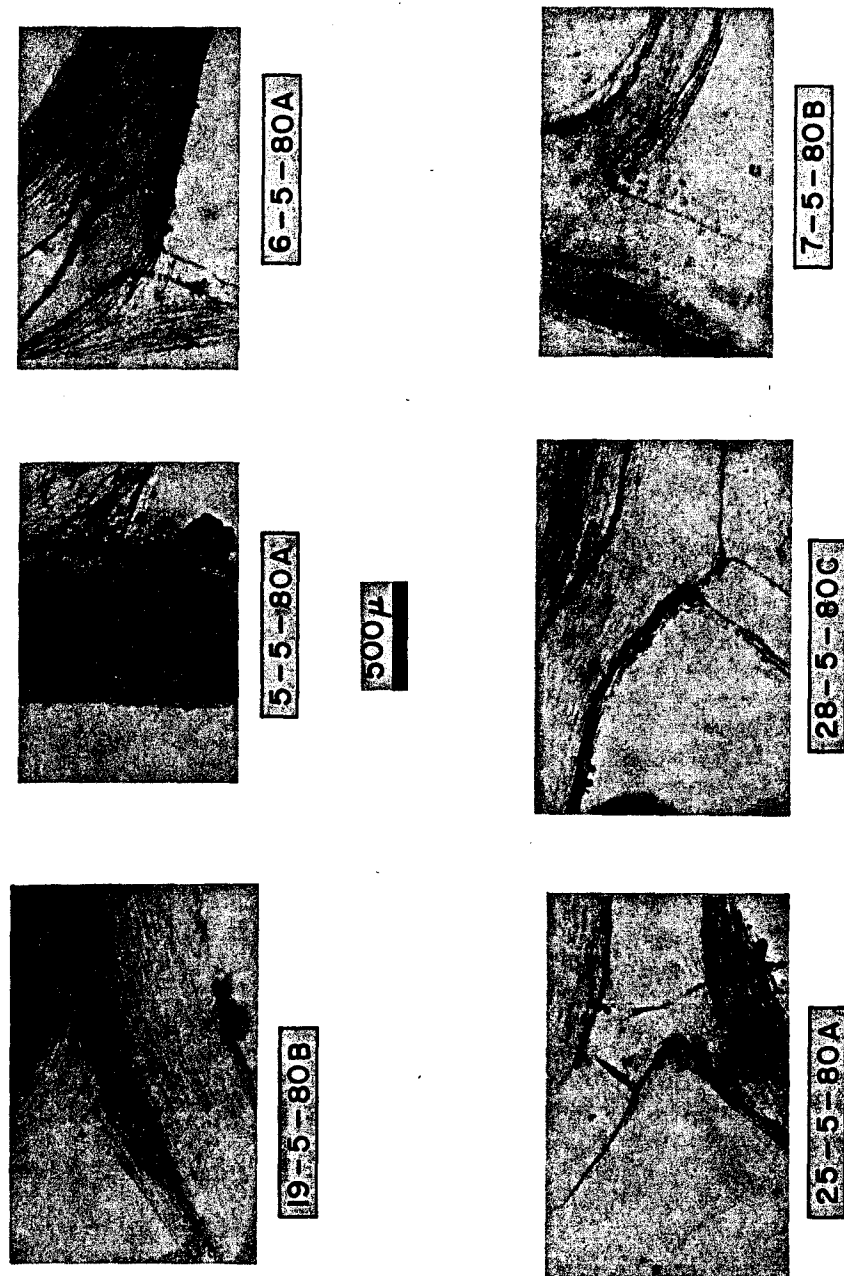


Fig. 2. Six typical branching geometries.

Temperature was monitored continuously throughout the experiments by a spherical thermistor (3 mm diameter) which had been previously calibrated against a standard glass laboratory thermometer. This thermistor was then located 1 mm from the axon at a point half way between the recording electrodes.

3. Differential pulse code transformations on straight axons

When the frequency of a train of nerve impulses becomes sufficiently high, the speed of an individual pulse decreases. This is because, at a sufficiently small time period between individual pulses, each is attempting to propagate into the relative refractory zone that follows in the wake of the preceding pulse. This effect has been studied numerically for the Hodgkin-Huxley (HH) axon by Rinzel (1979) and Miller and Rinzel (1981) who have shown that, to a rather good approximation, the speed of each impulse can be considered to depend only on the time interval separating it from the previous impulse. From a knowledge of the functional relation between pulse speed and pulse spacing, it is relatively simple to construct space-time trajectories for a train of impulses initiated at arbitrary times. The basis for this simple calculation is called 'pulse kinematics' by Miller and Rinzel.

Experimental measurements of the relationship between pulse speed and spacing have been published by Donati and Kunov (1976) and by us in the companion article (Scott and Vota-Pinardi, 1981). Both of these studies are of 'twin-pulse' experiments in which the speed of the second pulse is measured relative to that of the first. If the ratio of the second pulse speed to first pulse speed is called R and the time interval between them is called T , then the general form of the function $R(T)$ is as indicated on the 'fly-speck' diagram of Fig. 3. We have normalized all time intervals to the special time, T_1 , at which

$$(1) \quad R(T_1) = 1.$$

Fig. 3 epitomizes measurements made on fourteen different axons at various temperatures, and, although there is some variability in the data, the function $R(T)$ can be represented by the empirical relation

$$(2) \quad R = 1 + 0.105 \left(\frac{T}{T_1} - 1 \right) \exp \left[2.4 \left(1 - \frac{T}{T_1} \right) \right]$$

to an accuracy of about $\pm 5\%$.

From an inspection of Fig. 3 we can define three regions of pulse interval with broadly different dispersive properties:

Strongly dispersive region.—In this region $T < T_1$ and the following pulse has a speed much slower (up to 30–40% less) than that of its leader. This is because the propagation of the second is impeded by the relative refractory period left in the wake of the first.

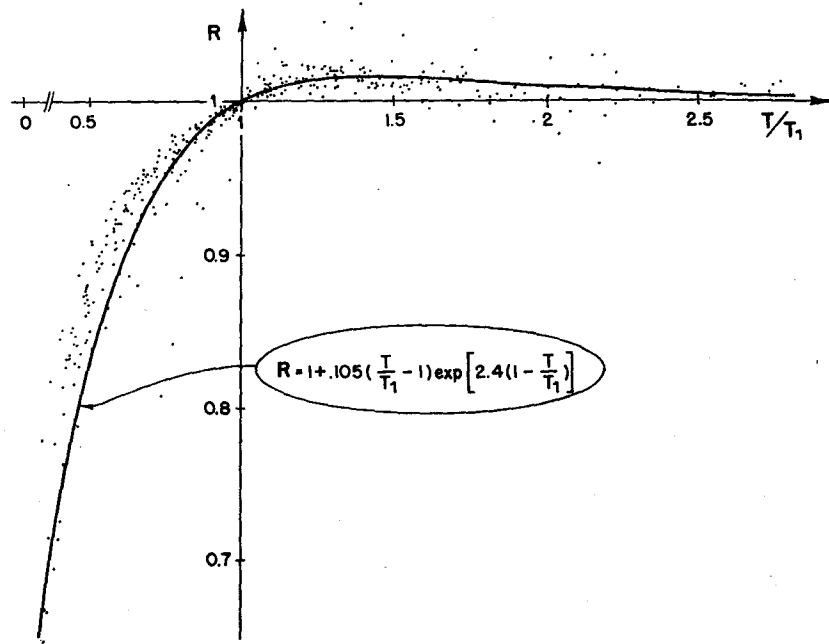


Fig. 3. The ratio of second pulse to first pulse speed (R) is plotted as a function of average pulse interval (T). Pulse interval is normalized with respect to the special value (T_1) at which R is equal to unity.

Weakly dispersive or 'supernormal' region.—Here pulse interval lies within the range $T_1 < T < 3T_1$ and the second pulse goes slightly faster (1–5% more) than the first. The second pulse speed is supernormal in this region because the tail of the first pulse has crossed over from inhibitory values below the resting level to excitatory values above.

Non-dispersive region.—For a pulse interval greater than about $3T_1$, no dispersive effects are observed.

In Fig. 4 we display values of T_1 vs. the temperatures at which they were measured and compare these data with numerical computations by Miller and Rinzel (1981) for the Hodgkin–Huxley (HH) equations. Both calculations and data have a temperature dependence of about

$$(3) \quad T_1 \propto 3^{-\text{Temp}/10}$$

as is to be expected if the dispersion is governed by HH recovery dynamics. However, the calculated temperature dependence is slightly less steep than that indicated in (3) while the experimental dependence is, if anything, slightly more steep. Furthermore the measured data exceeds the calculations by a factor that

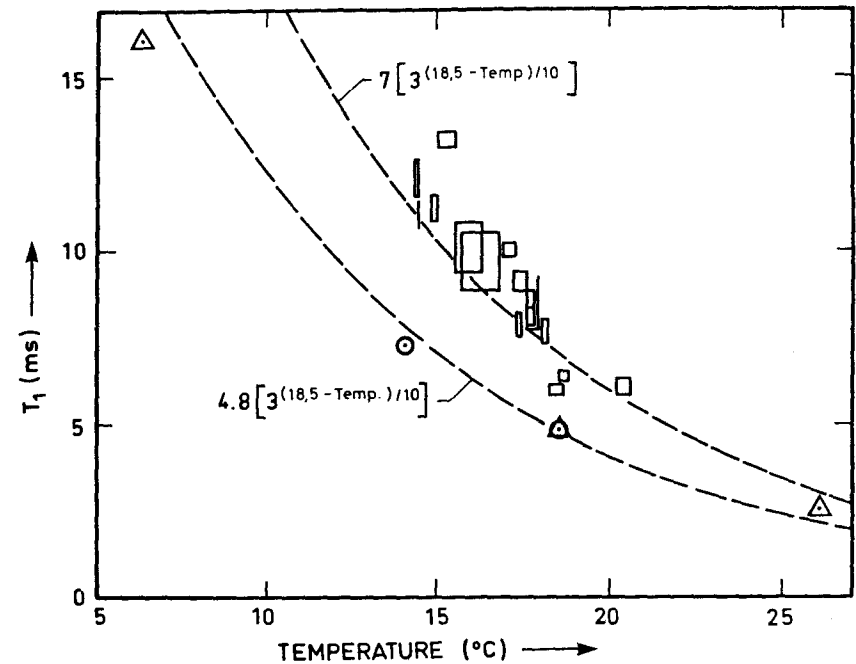


Fig. 4. Measured values of T_1 vs. temperature. The points \circ were calculated by J. Rinzel for the HH equations with twin-pulse stimulation. The points Δ were calculated by Miller and Rinzel (1981) for periodic stimulation.

ranges from 1.5 at 20°C to 1.75 at 14°C. This is a rather large discrepancy for which we can suggest two general explanations.

(1) *Systematic errors in the measurement of temperature.*—Such errors could arise because the temperature measuring thermistor could be located only at one point along the axon (half way between recording electrodes) and the temperature near the recording electrodes may have been different. Also the thermal environment of the thermistor during measurement may have been different from that during calibration.

(2) *Real differences between the axons studied and the Hodgkin–Huxley model.*—An important dynamic effect not included in the original HH equations has been described by Frankenhaeuser and Hodgkin (1956) and attributed to the transient accumulation of potassium ions in the periaxonal space just outside the membrane. Using a modified version of the HH equations that accounts for this depolarizing effect (Adelman and Fitzhugh, 1975), George and Silberstein (1977) show that the maximum value of R in a twin-pulse measurement is reduced. We expect that a decrease in the maximum value of R should lead to a larger value for T_1 . Other

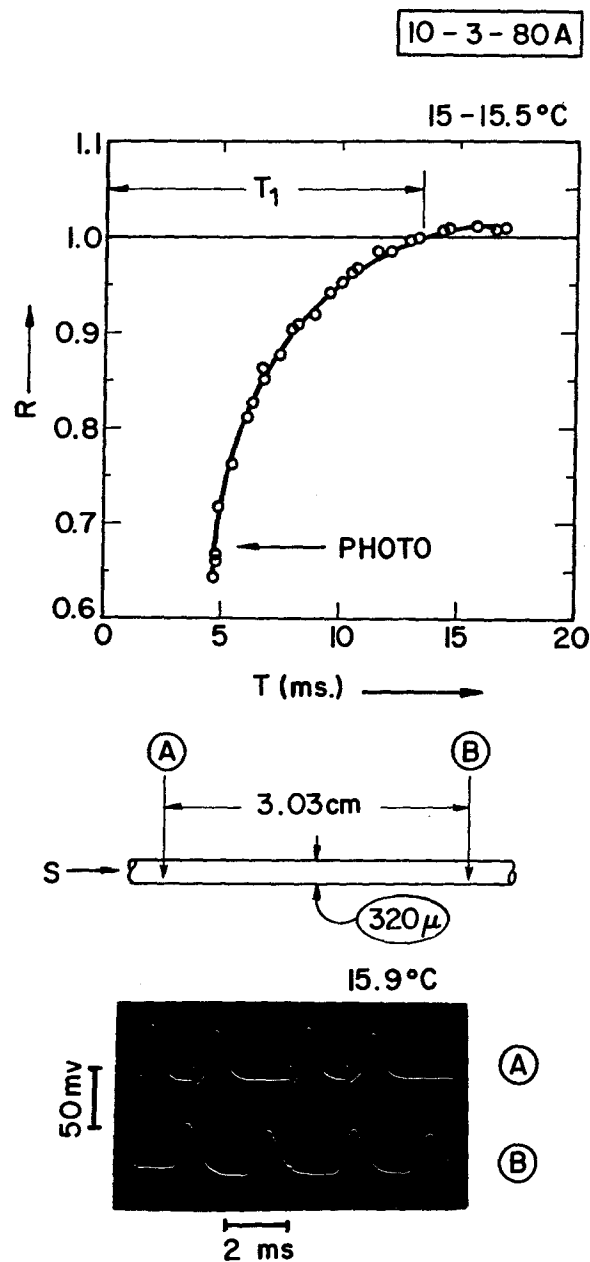


Fig. 5. Velocity dispersion and frequency smoothing on a straight axon.

discrepancies between our measurements and HH calculations might be ascribed to biological differences between the *Loligo vulgaris* of Naples and the *Loligo* from Plymouth studied by Hodgkin and Huxley (1952).

It seems unlikely to us that all of the differences between measurements and HH computations displayed in Fig. 4 should be assigned to errors in temperature measurement; however, we are presently unable to determine how much is temperature error and how much is due to real differences between our axons and the HH model.

As Miller and Rinzel (1981) and Rinzel (1979) have shown, one result of stimulating in the strongly dispersive region with a pulse train that does not have equal intervals is a 'frequency-smoothing' effect. Pulse intervals initially unequal tend to become equal as the smaller intervals increase and the larger ones decrease. This effect is shown in Fig. 5 where we have plotted $R(T)$ with T defined as the average of the time delays measured for the first and the second impulses. From the CRO record, first pulse delay is about 2.2 ms and second pulse delay is about 3.2 ms so the speeds of the second and fourth pulses are about 32% less than that of the first and third. These velocity variations cause the time intervals between first and second (and third and fourth) pulses to increase while the interval between the second and third impulse decreases. Thus the pulse train observed on the downstream electrode (B) is much closer to a single frequency than that observed on the upstream electrode (A). This dynamical effect is quite similar to that displayed in Fig. 5c of Rinzel (1979).

4. Quantum pulse code transformations

Here we describe dynamic events in which nerve impulses are suddenly lost as they attempt to propagate through regions where the nerve fiber bifurcates (or branches). As Rall (1959) has shown, one aspect of the difficulties faced by such impulses is expressed as the *geometrical ratio* (GR) of the branch. This ratio is essentially the characteristic admittance of out-going fibers divided by that carrying the incoming pulse, and, in terms of fiber diameters (d), it takes the form

$$(4) \quad GR = \frac{\sum d_{OUT}^{3/2}}{d_{IN}^{3/2}}.$$

If $GR = 1$, the 'impedance matching' between outgoing and incoming fibers is perfect and a pulse should proceed through the branch with a minimum of difficulty. As GR becomes progressively greater than 1, difficulties increase. Numerical calculations based on the HH model axon indicate that for GR equal to 10 or 11 a solitary impulse will fail to propagate through the bifurcation (Berkinblit *et al.* 1970; Parnas and Segev, 1979).

A histogram of the orthodromic GR 's for 109 bifurcations is displayed in Fig. 6. It should be emphasized that these bifurcations include rather equal representations of all the different daughter diameter ratios shown in Fig. 2; thus it seems that in

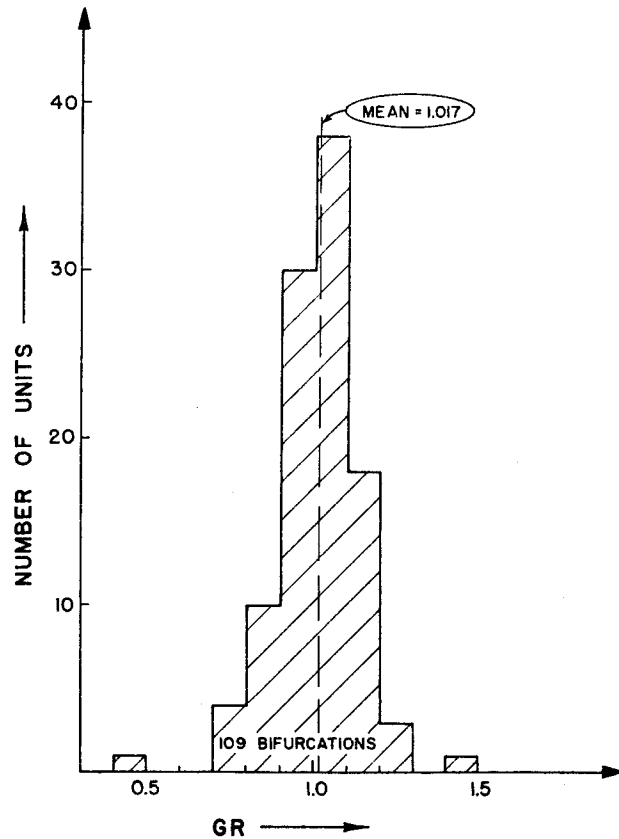


Fig. 6. Histogram of orthodromic GR's.

the squid axon nature is attempting to match impedances under a variety of geometrical constraints.

We examined sixteen bifurcations under orthodromic stimulation seeking evidence for a change in temporal pulse code before and after the bifurcation. Although such a change was sometimes observed, we failed to find any case for which surgical damage or the effect of tiring the axon during the search could be eliminated. Thus we turned to antidromic stimulation in order to increase the *GR*. An example of a pulse code transformation that was then observed on a fresh preparation is shown in Figs 7 and 8. The bifurcation geometry (Fig. 7a) indicates that for stimulation on branch B of 29-2-80B

$$GR = 2.14.$$

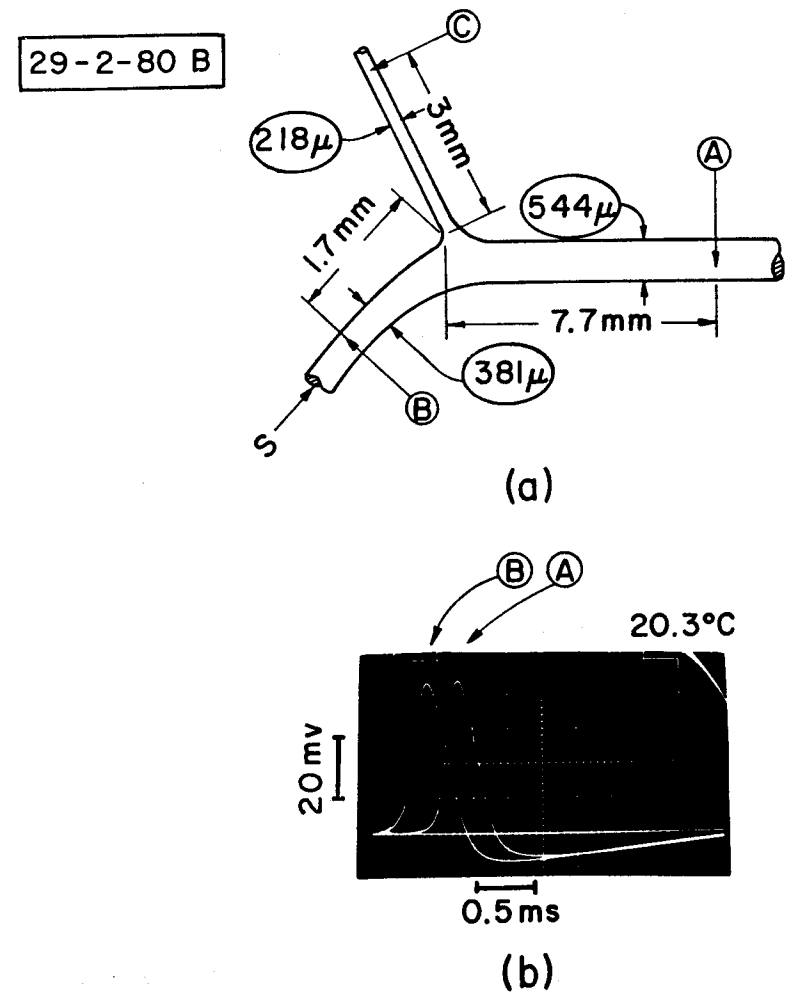


Fig. 7. (a), Branching geometry and (b), single action potentials.

Fig. 7b shows the propagation of a solitary impulse through the bifurcation. In Fig. 8 the stimulation was a double pulse at a level 2.6 times threshold. This figure shows a critical adjustment of experimental parameters such that the second pulse just fails (upper photo) or just makes it through the bifurcation (lower photo).

When the second pulse passes through the bifurcation, it produces an artifact (or 'hump') on the upstream (B) record. The observation of this hump is important

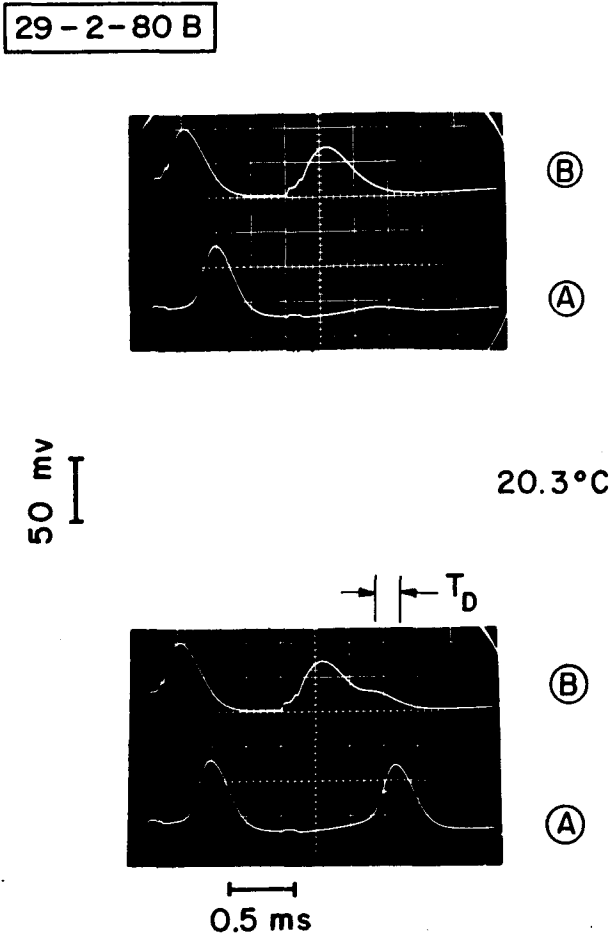


Fig. 8. With twin-pulse stimulation of the preparation described in Fig. 7 the second pulse fails (upper) and passes (lower).

because it permits us to locate the critical dynamic event that reproduces the second pulse. This location proceeds as follows. We have observed a dependence of conduction velocity (θ) upon axon diameter (d) and temperature (to within a few per cent) as

$$(5) \quad \theta = \left[\frac{d}{476} \right]^{1/2} [2.03 + 0.078(\text{Temp} - 18.5)], \text{ cm/ms.}$$

From Eq. (5) we can calculate the time of delay for a solitary pulse to go from the crotch of the bifurcation to electrode (A); we call this T_A . Likewise T_B is calculated

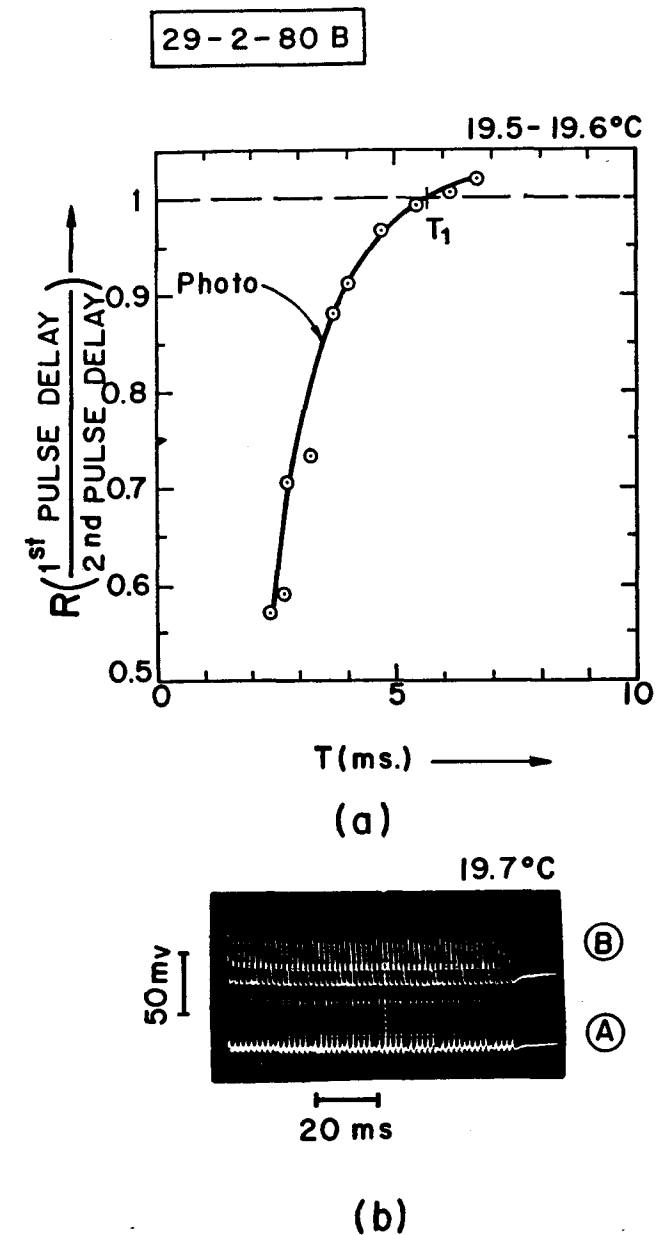


Fig. 9. (a), Dispersion curve and (b), pulse code transformation in the preparation of Fig. 7.

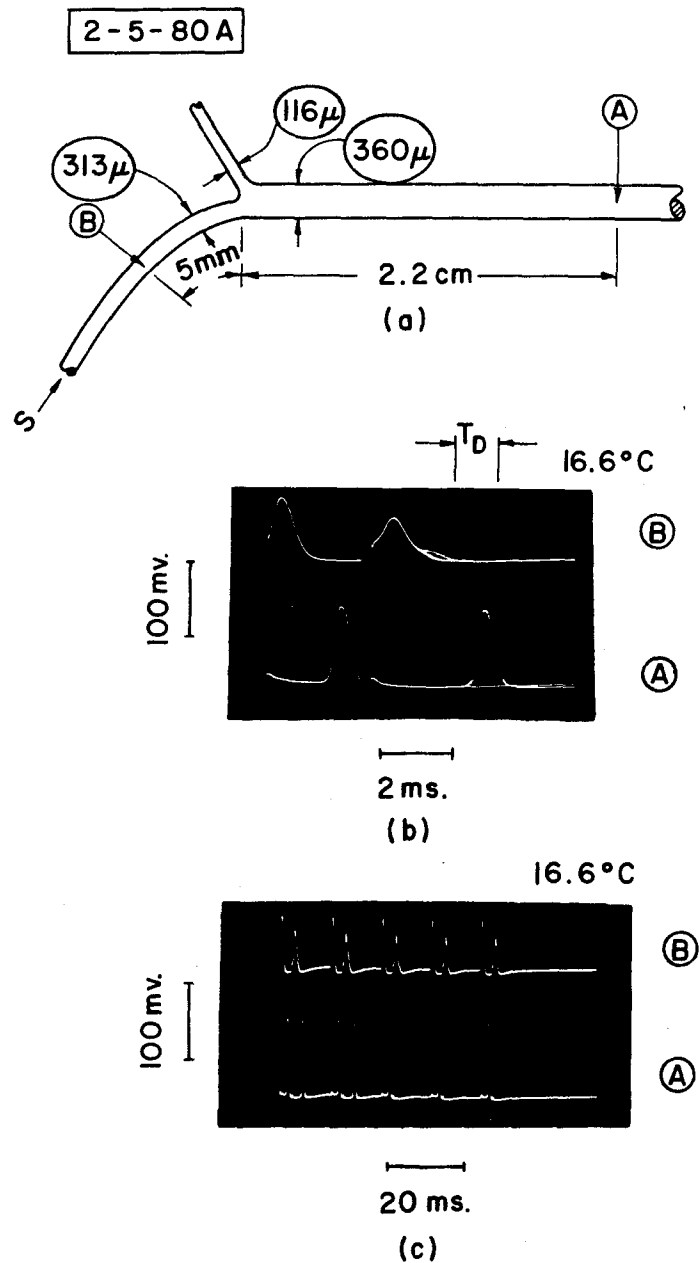


Fig. 10. (a) Branching geometry for which (b), the critical twin-pulse effect was observed. (c) A quantum pulse code transformation.

as the time for a pulse to travel backward from the crotch to electrode (B). The total time delay, T_D , between the second pulse and the hump is greater than $T_A - T_B$ because the time interval between the two pulses is within the 'strongly dispersive region' as defined above. Thus if the second impulse is triggered at the bifurcation, we expect

$$(6) \quad T_D = (T_A - T_B)/R.$$

With the parameters appropriate for Fig. 8 we find

$$T_D = \begin{cases} 0.38 \text{ ms} & (\text{calculated}), \\ 0.35 \text{ ms} & (\text{measured}). \end{cases}$$

A difference of 0.03 ms between calculated and measured delays locates the critical dynamic event to within about half a millimeter of the bifurcation. In any case, the difference between measured and calculated values of T_D is somewhat less than uncertainties in T_A , T_B and R , and commensurate with the precision to which T_D can be measured.

Fig. 9b shows a typical example of pulse code translation at an incoming pulse rate of 300 pps which corresponds to the pulse interval of 3.3 ms indicated on the dispersion curve of Fig. 9a. At the end of our measurements on 29-2-80B we recorded simultaneously from (A) and (C) (while stimulating on the larger daughter) and observed different pulse codes. However, by this time the preparation had been fatigued by measurements of dispersion and the search for interesting examples of pulse code transformation.

In Fig. 10 we display results for 2-5-80A under antidromic stimulation of the larger daughter. Fig. 10b is a multiple trace photograph which clearly shows the relation between time delay of the hump and that of the second pulse. The correspondence between measured and calculated values of T_D is

$$T_D = \begin{cases} 1.30 \text{ ms} & (\text{calculated}), \\ 1.40 \text{ ms} & (\text{measured}). \end{cases}$$

Again the difference between these two numbers is commensurate with the precision to which they have been determined and they locate the critical dynamic event to within two millimeters of the bifurcation.

We have made a search for the critical value of pulse interval at which the second pulse just makes it through the bifurcation on twelve different preparations. In each case we looked first for this critical effect so our observations are entirely on fresh preparations stimulated no more than a dozen or two times. Of these twelve preparations, we were able to find a critical pulse interval for four. Our results are displayed in Fig. 11 which indicates both the time interval, T , between incident impulses and the corresponding geometric ratio. Cases in which the critical pulse interval was observed are shown as '○' on the diagram. Cases for which we could not find a critical interval are indicated as '←' because we suppose it might be found at a smaller value of T than we were able to achieve. We expect, of course, that the critical value of pulse interval should depend upon the time, T_1 ,

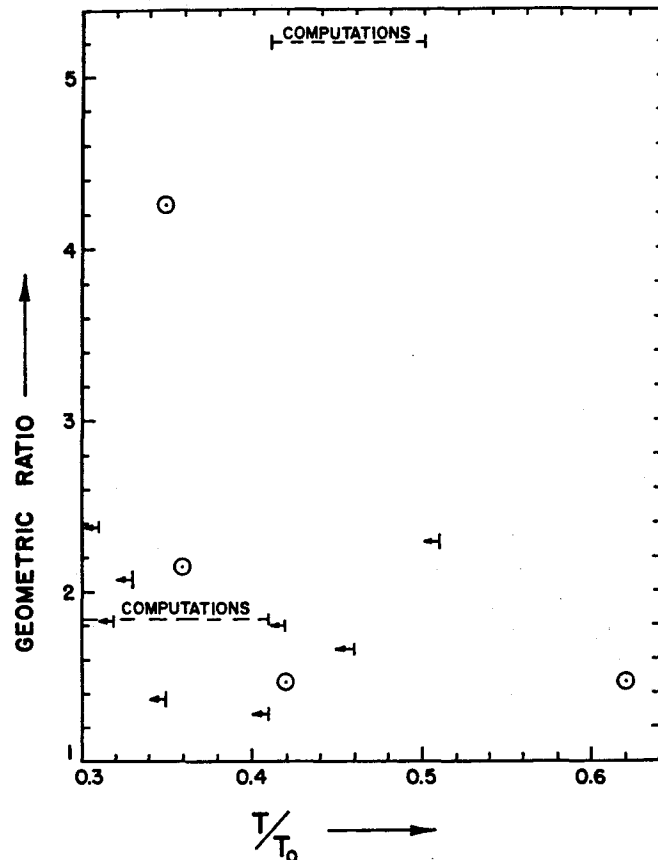


Fig. 11. Comparison of geometric ratio and pulse interval at which the critical twin-pulse effect (as in Figs 8 and 10b) was observed. Note that T_0 is approximately equal to T_1 in Fig. 3. Computations are from Khodorov *et al.* (1971).

below which strong dispersion is observed. Thus it seems reasonable in the display of Fig. 11 to normalize observed times to T_1 . Actually, we found it experimentally more convenient to normalize with respect to the time interval between the threshold of a solitary pulse and the first 'cross-over' of its tail through the resting value. We call this 'cross-over' time T_0 and have shown in Scott and Vota-Pinardi (1982) that $T_0 \approx T_1$.

The measured values of time delay between the hump and the second impulse are compared in Fig. 12 with values calculated from Eq. (6).

Another type of pulse code transformation is shown in Figs 13 and 14 for bifurcation number 20-3-80A; under antidromic stimulation on the larger

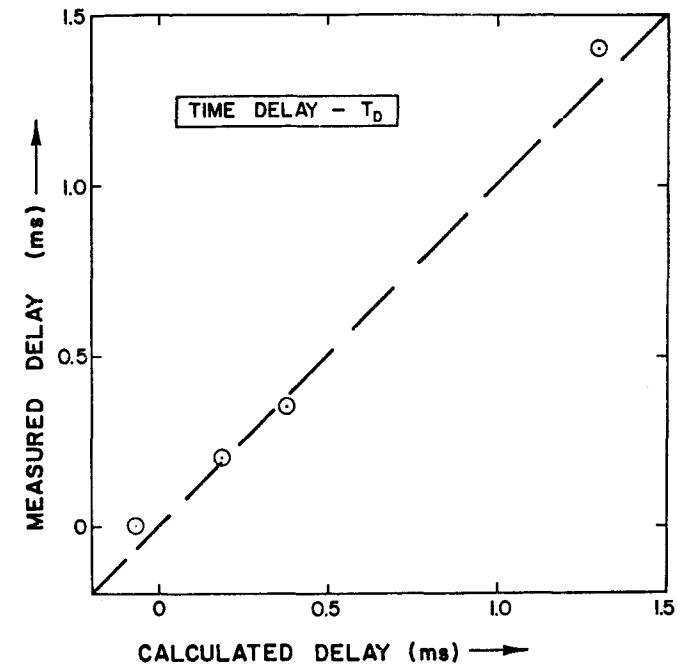


Fig. 12. Comparison of measured time delay (T_D) between hump and second impulse (see Figs 8 and 10b) with calculations from Eq. (6).

daughter, $GR = 1.71$. Stimulating with a pulse rate of 160 pps in a single burst of one half second, the outgoing pulse train gradually changed, over 220 ms, to a pulse rate of 80 pps. This effect was observed on several preparations and, for a particular preparation, was quite stable and reproducible. We wish to emphasize that such a delayed pulse code transformation is not considered in the results displayed in Fig. 11; there only the loss of the second of *two* pulses was recorded.

Observations of an isolated dynamic effect observed for axon number 5-2-80B are shown in Figs 15 and 16. This was essentially a straight axon and we made measurements of pulse speed vs. frequency for a short burst (3 or 4) of pulses. At a pulse rate slightly more than 100 pps we were forced to stop these measurements because (as Fig. 16b shows) one of the downstream pulses was missing. Subsequent investigation revealed the situation shown in Fig. 16c where at an incoming pulse rate of 150 pps a downstream pulse (B) appeared only when an upstream pulse (A) was missing. A very careful examination of the axon both that evening and the following morning revealed only the small cut branch sketched in Fig. 15a as a possible cause for such unexpected behavior.

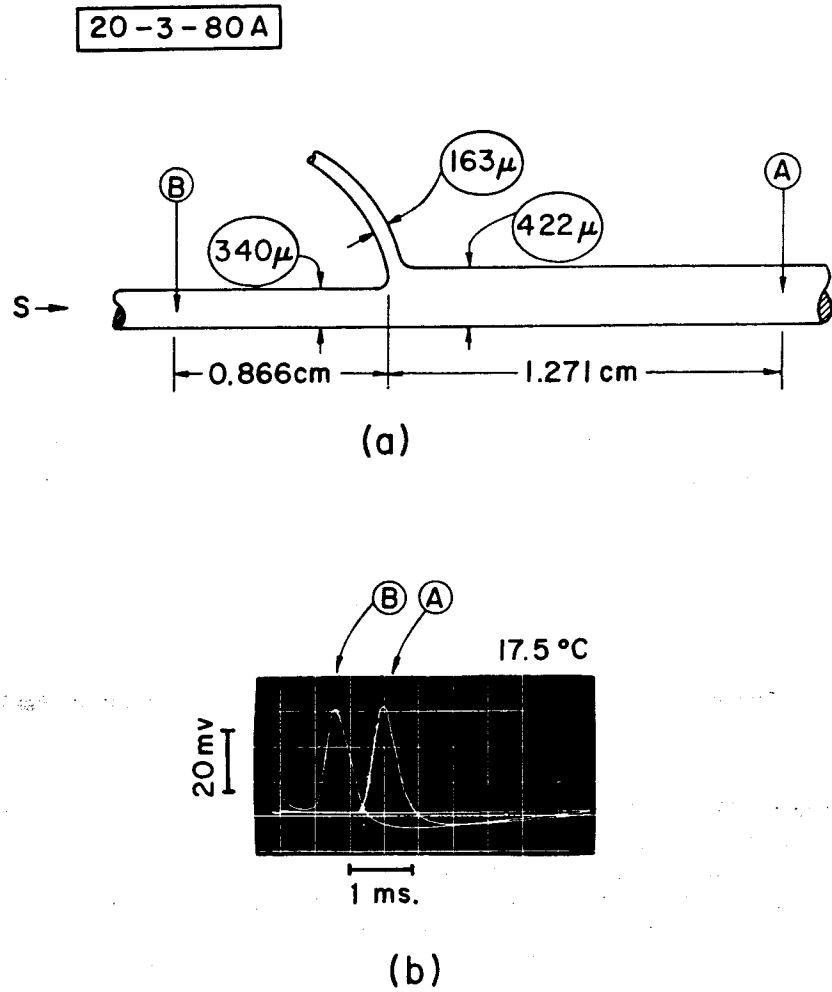


Fig. 13. Branching geometry and single action potentials.

5. Discussion

One might suppose that a condition to observe the pulse kinematics described in connection with Fig. 5 would be to have an axon long enough to support both interacting pulses. From Eq. (5), however, we find a pulse velocity of about 1.5 cm/ms ; and from Fig. 5 the time occupied by two pulses is about 7 ms . Thus the corresponding distance is about 10 cm which is longer than the axon. The interelectrode distance of 3 cm , on the other hand, corresponds to 2 ms or just

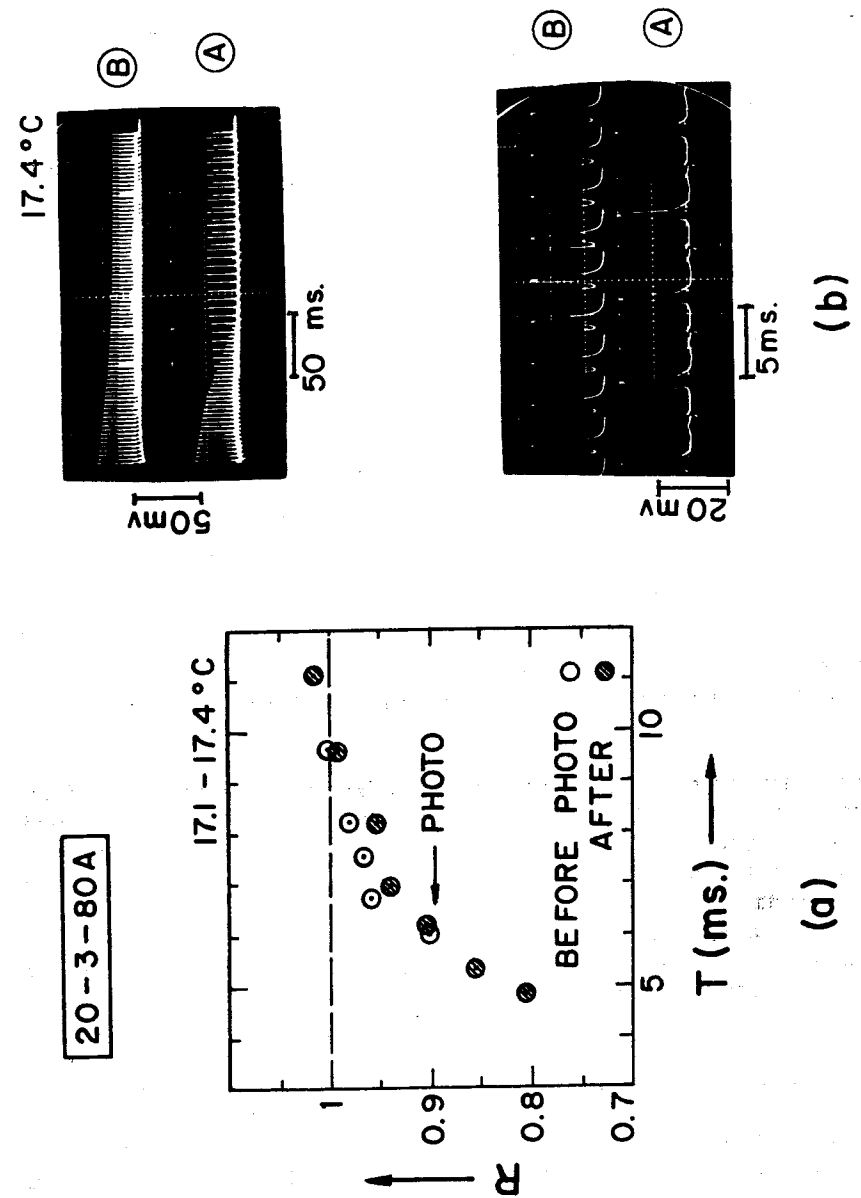


Fig. 14. (a), Dispersion diagram and (b), slow onset of QPT for the preparation of Fig. 13.

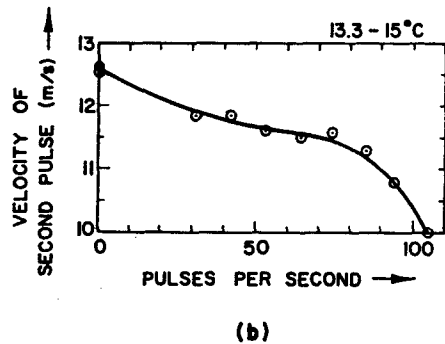
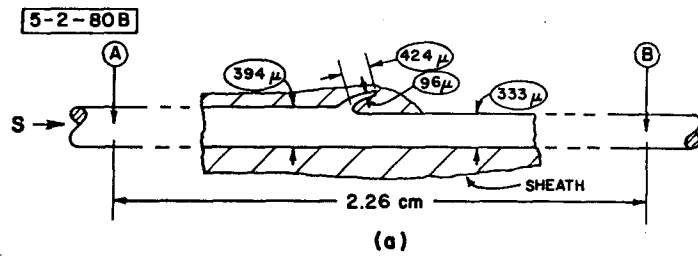


Fig. 15. (a), Straight axon with small lateral branch and (b), velocity vs. pulse rate.

one square of the CRO photograph in Fig. 5. From the theoretical study of dispersion in Scott and Vota-Pinardi (1981), however, it is clear that the axon need only be long compared with the region of interaction between the tail of one pulse and the leading edge of a following pulse. For Fig. 5 this is a time of 1 ms or an axon length of 1.5 cm.

We find a region of weak dispersion in which pulse velocity is slightly greater than that of an isolated pulse for an interval T between T_1 and $3T_1$. In terms of temperature this condition becomes

$$(7) \quad 5 < T[3^{(\text{Temp} - 18.5)/10}] < 21 \text{ ms.}$$

This is a considerably smaller range of 'supernormality' than has been observed in several other experiments (Graham, 1934; Bullock, 1951; Gardner-Medwin, 1972; Swadlow and Waxman, 1976; George, 1977; Bliss and Rosenberg, 1979) although Kocsis *et al.* (1979) have observed a T_1 of 1.7 ms on visual cortical efferent neurons of the rabbit.

Since the squid bifurcations we investigated all had orthodromic $GR < 1.3$ (see Fig. 6) and no examples of quantum pulse code transformations were observed

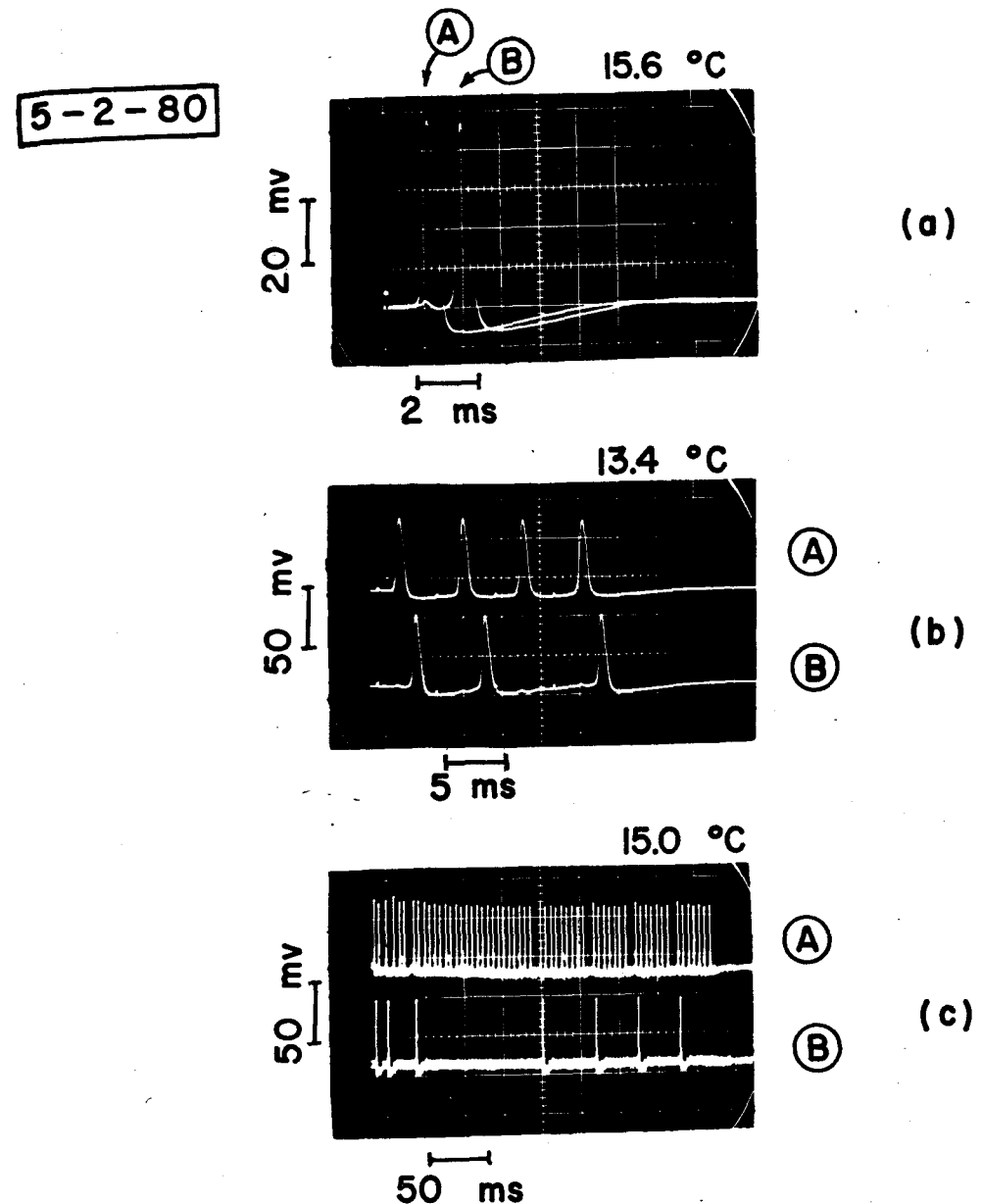


Fig. 16. For the preparation of Fig. 15: (a), single action potentials, (b), QPT, and (c), 'NOT' function [see Eq. (8)].

for $GR < 1.4$ (see Fig. 11), we feel it is unlikely that normal squid axon bifurcations could process information via quantum pulse code transformations without the assistance of some prolonged stimulation effects. This is consistent with recent conclusions by Smith (1980) that are based on observations of branching axons from crayfish.

A difficulty in relating quantum pulse code transformations to bifurcation geometry is to ensure that pulses are being blocked at the bifurcation and not as a result of some surgical damage to the axon during its removal from the mantle. Our technique to locate the critical event in double pulse antidromic experiments (Fig. 11) was to calculate the time delay, T_D , between hump and second pulse from Eq. (6) and compare it with measured values (see Figs 8 and 10). The measured and calculated values of this delay, displayed on Fig. 12, indicate agreement within experimental precision and locate the critical event within a millimeter or two from the crotch of the bifurcation. Within this region a careful microscopic examination for 'other causes' was quite feasible. Thus we are rather certain that the four observations indicated by '○' on Fig. 11 show the effect of bifurcation geometry on double pulse transmission.

On the plot of Fig. 11 we expected to find a locus of critical observations on the boundary of a (right-hand) region of second pulse passage and a (left-hand) region of second pulse block. The locus of this boundary is given for the HH axon in an approximate way by the computations of Khodorov *et al.* (1971). Clearly more data are needed, but three of our four critical points lie close to the region where the numerically computed boundary is found. Fig. 11 exemplifies one general statement about our observations of quantum pulse code transformations: such effects were only found in the strongly dispersive region.

Scatter in the data plotted on Fig. 11 could be caused in at least two ways. (1) Uncontrolled variability in the detailed properties of the bifurcation (e.g. partial removal of sheath, non-uniform density of sodium or potassium channels, etc.), or (2), variation in the delay ratio (see R in Fig. 3) as a function of T/T_0 . We plan to investigate this question more carefully in future work.

It should be emphasized that most of our measurements were made with the intent to avoid effects of prolonged stimulation. Generally we were able to arrange a preparation for measurements with no more than a dozen or two isolated stimulations. During measurements, the stimulations were triggered manually when needed. Observations of the sort displayed in Fig. 14, for example, were made only after all the twin-pulse data had been taken. Since the time constants for effects as in Fig. 14b were between 50 and 100 ms, we suppose that the mechanism may be related to potassium accumulation in the periaxonal space (Frankenhaeuser and Hodgkin, 1956; Adelman and Fitzhugh, 1975; Smith and Hatt, 1976; Grossman *et al.*, 1979a,b; Smith, 1980a,b).

The essential dynamic behavior exhibited by axon number 5-2-80B in Fig. 16c is that a missing pulse on the upstream code (A) causes a pulse to appear on the downstream code (5). In the language of computer science, this behavior can be described by the Boolean function

$$(8) \quad B = \text{NOT}(A).$$

Such an effect is interesting because the 'NOT' function together with the previously established 'AND' and 'OR' functions permits the synthesis of an arbitrary logical computation (Scott, 1977). However, it is unlikely that the behavior in Fig. 16c is physiological; it seems rather to be pathologically related to the effect of a small cut fiber shown in Fig. 15a.

6. Conclusions

(1) From fourteen twin-pulse experiments, a plot of velocity ratio (R) against normalized pulse interval (T/T_1) (see Fig. 3) yields the approximate dispersion formula, Eq. (2). (The time, T_1 , was defined in a companion work (Scott and Vota-Pinardi, 1982) as the pulse interval at which both pulses have the same speed.)

(2) For a pulse interval $T < T_1$, we find a region of 'strong dispersion' in which the second pulse travels more slowly than the first. For a pulse interval $T_1 < T < 3T_1$, we find a weakly dispersive or 'supernormal' region in which the second pulse travels faster than the first. For $T > 3T_1$, no dispersion effects are observed.

(3) Temperature dependence of T_1 is approximately as the Hodgkin-Huxley factor $3^{-T_{\text{emp}}/10}$ between 14°C and 21°C.

(4) Quantum pulse code transformations (QPT) (i.e. sudden loss of one or more action potentials) were observed only in the strongly dispersive region.

(5) The orthodromic GR 's of 109 bifurcations had a mean value of 1.017, all but two lying between 0.7 and 1.3.

(6) No reliable evidence was obtained for QPT at the bifurcation under orthodromic stimulation of fresh preparations.

(7) With twin-pulse stimulation of twelve fresh preparations having antidromic GR 's between 1.28 and 4.25, four showed QPT. These four events were located at the bifurcations.

Acknowledgements

We wish to express our appreciation to the staff at the Stazione Zoologica in Naples for their help during the course of this work, and particularly to the Director, Professor A. Monroy for his warm hospitality and to Dr. A. De Santis for encouragement and advice during the early stages. Special thanks to L. MacNeil for technical assistance and to Dr. J. Rinzel for helpful discussions and special numerical computations. One of us (ACS) was supported by a Senior Fellowship from the European Molecular Biology Organization. The Consiglio Nazionale delle Ricerche (Italy) provided certain test equipment and supplies, and the National Science Foundation (U.S.) supported preparation of the manuscript.

References

- Adelman, W. J., Jr. and Fitzhugh, R. (1975). Solutions of the Hodgkin-Huxley equations modified for potassium accumulation in a periaxonal space. *Fed. Proc.* **34**, 1322-1329.

- Berkinblit, M. B., Vvedenskaya, L. S., Gvedenko, S. A., Kovalev, A. V., Kholopov, S. V., Formin, S. V. and Chailakhyan, L. M. (1970). Computer investigation of the features of conduction of a nerve impulse along fibers with a different degree of widening. *Biophysics* **15**, 1121-1130.
- Bliss, T. V. P. and Rosenberg, M. E. (1979). Activity dependent changes in conduction velocity in the olfactory nerve of the tortoise. *Pflügers Arch.* **381**, 209-216.
- Bullock, T. H. (1951). Facilitation of conduction rate in nerve fibers. *J. Physiol.* **114**, 89-97.
- Donati, F. and Kunov, H. (1976). A model for studying velocity variations in unmyelinated axons. *IEEE Trans. Biomed. Eng.* **BME-23**, 23-28.
- Frankenhaeuser, B. and Hodgkin, A. L. (1956). The after-effects of impulses in the giant nerve fibers of *Loligo*. *J. Physiol.* **131**, 341-376.
- Gardner-Medwin, A. R. (1972). An extreme supernormal period in cerebellar parallel fibers. *J. Physiol.* **222**, 357-371.
- George, S. A. (1977). Changes in interspike interval during propagation: quantitative description. *Biol. Cybernetics* **26**, 209-213.
- George, S. A. and Silberstein, P. T. (1977). Conduction velocity after-effects of spike activity. *Neuroscience Abstr.* **3**, 217.
- Graham, J. T. (1934). Supernormality, a modification of the recovery process in nerve. *Am. J. Physiol.* **110**, 225-242.
- Grossman, Y., Parnas, I. and Spira, M. E. (1979a). Differential conduction block in branches of a bifurcating axon. *J. Physiol.* **295**, 283-305.
- Grossman, Y., Parnas, I., and Spira, M. E. (1979b). Ionic mechanisms involved in differential conduction of action potentials at high frequency in a branching axon. *J. Physiol.* **295**, 307-322.
- Hodgkin, A. L. and Huxley, A. F. (1952). A quantitative description of membrane current and its application to conduction and excitation in nerve. *J. Physiol.* **117**, 500-544.
- Khodorov, B. I., Timin, Ye. N., Pozin, N. V. and Shemelev, L. A. (1971). Conduction of a series of impulses through a portion of the fiber with increased diameter. *Biophysics* **16**, 96-104.
- Kocsis, J. D., Swallow, H. A., Waxman, S. G. and Brill, M. H. (1979). Variation in conduction velocity during the relative refractory period and supernormal periods: a mechanism for impulse entrainment in central axons. *Exptl. Neurol.* **65**, 230-236.
- Miller, R. N. and Rinzel, J. (1981). The dependence of impulse propagation speed on firing frequency, dispersion, for the Hodgkin-Huxley model. *Biophys. J.* **34**, 227-259.
- Parnas, I. and Segev, I. (1979). A mathematical model for conduction of action potentials along bifurcating axons. *J. Physiol.* **295**, 323-343.
- Rall, W. (1959). Branching dendritic trees and motoneuron membrane resistivity. *Exptl. Neurol.* **1**, 491-527.
- Rinzel, J. (1979). Impulse propagation in excitable systems. *Proc. Math. Res. Center Advanced Seminar on Dynamics and Modelling of Reactive Systems*. U. of Wisconsin, Madison.
- Scott, A. C. (1977). *Neurophysics*. Wiley, New York.
- Scott, A. C. and Vota-Pinardi, U. (1982). Velocity variations on unmyelinated axons. *J. Theoret. Neurobiol.* **1**, 150-172.
- Smith, D. O. (1980a). Mechanisms of action potential propagation failure at sites of axon branching in the crayfish. *J. Physiol.* **301**, 243-259.
- Smith, D. O. (1980b). Morphological aspects of the safety factor for action potential propagation at axon branch points in the crayfish. *J. Physiol.* **301**, 261-269.
- Smith, D. O. and Hatt, H. (1976). Axon conduction block in a region of dense connective tissue in crayfish. *J. Neurophysiol.* **39**, 794-801.
- Swadlow, H. A. and Waxman, S. G. (1976). Variations in conduction velocity and excitability following single and multiple impulses of visual callosal axons in the rabbit. *Exptl. Neurobiol.* **53**, 128-150.
- Waxman, S. G. (1972). Regional differentiation of the axon: a review with special reference to the concept of the multiplex neuron. *Brain Res.* **47**, 269-288.